Macromolecules
ARTICLE

Macromolecules **2010**, *43*, 5411–5416 **5411**
DOI: 10.1021/ma1003419

SANS Investigation of Selectively Distributed Single-Walled Carbon Nanotubes in a Polymeric Lamellar Phase

Changwoo Doe,[†] Hyung-Sik Jang,[†] Steven R. Kline,[‡] and Sung-Min Choi*,[†]

[†]*Department of Nuclear and Quantum Engineering, Korea Advanced Institute of Science and Technology, Daejeon, 305-701, Republic of Korea, and* [‡]*NIST Center for Neutron Research, Gaithersburg, Maryland 20899-6102*

Received February 11, 2010; Revised Manuscript Received May 3, 2010

ABSTRACT: Fabrication of highly ordered superstructures of single-walled carbon nanotubes (SWNTs) is of great interest for a wide range of potential applications. Here, we investigate the selective distribution of individually isolated SWNTs (1D nanoparticles with very large aspect ratios) in Pluronic P84/water/*p*-xylene ternary systems in a lamellar phase by contrast variation small-angle neutron scattering measurements. Hydrophilically functionalized SWNTs (*p*-SWNTs) with an aspect ratio of ca. 100 are mixed with P84/water/*p*-xylene systems prepared with two opposite neutron contrasts, a positive contrast for which the neutron scattering length density of the apolar domain is higher than that of the polar domain and a negative contrast for which the relative scattering length density is opposite. The neutron scattering intensity of the first-order Bragg peak, after correcting for the effect of *p*-SWNT-induced diffuse interface, increases with addition of *p*-SWNTs in the positive contrast samples and decreases in the negative contrast samples. This shows that *p*-SWNTs, of which the length is ca. 70 times larger than the thickness of polar domain while its diameter is comparable to the polar domain thickness, are selectively distributed in the polar domains of the P84/water/*p*-xylene lamellar phase.

Introduction

Self-assembly of 1D nanoparticles into highly ordered superstructures has been of great interest for potential applications in developing new functional hybrid materials.[1−3] Single-walled carbon nanotubes (SWNTs) are one of the most promising 1D nanoparticles in the field of nanotechnology for their remarkable mechanical, electrical, and thermal properties[4,5] which are the basis for a wide range of applications such as nanoscale electronic devices,[6,7] sensors,[8−10] energy storage materials,[11,12] and reinforcement materials.[13,14] However, realization of the potential applications of SWNTs is still at an early stage.[15] One of the difficulties that hinders practical applications of SWNTs is the lack of simple and effective methods to fabricate SWNT superstructures with desired morphology and orientations. As an effort to achieve such SWNT superstructures, for example, SWNT structures with preferential orientation have been successfully demonstrated using methods such as evaporation,[16,17] electric field,[18] or spin coating.[7] In spite of these successful demonstrations showing preferentially oriented SWNTs, an easy and simple method to fabricate SWNT superstructures of versatile geometries is yet to be developed.

Block copolymers exhibit rich phase behavior and have been extensively used as excellent templates for nanostructured materials.[19−22] Recently, there have been many efforts to incorporate nanoparticles[23] such as spherical gold[24,25] and CdSe[26] nanoparticles or gold nanorods[27] into self-assembled block copolymers to efficiently fabricate patterned nanoparticle−polymer composites or to improve physical properties of the composite materials. In these examples, the equilibrium location and distribution of nanoparticles in bulk block copolymers were determined by the selective interaction[25−27] between nanoparticles and specific blocks of the block copolymers and the size[24,28] of the nanoparticles. Theoretical studies also predict that the cooperative self-assembly of functionalized nanoparticles and block copolymers can provide a wide variety of nanoparticle−polymer composites with well-controlled particle arrangements.[28−31] While patterned nanoparticle−polymer composites have been achieved via self-assembly for nanospheres or nanorods with relatively small aspect ratios, however, controlled and guided distribution of one-dimensional nanoparticles with very large aspect ratios such as SWNTs in polymeric systems has not been fully exploited yet.

In this study, we have investigated the selective distribution of SWNTs in the Pluronic P84 ($PEO_{19}PPO_{43}PEO_{19}$)/water/*p*-xylene ternary system[32] in the lamellar phase by contrast variation small-angle neutron scattering (SANS) measurements. The surfaces of individual SWNTs are hydrophilically functionalized via in situ polymerization of surfactant monolayers encapsulating SWNTs,[33] which provide selective affinity to the hydrophilic domains of the ternary system. Therefore, selective distribution of individually isolated SWNTs in the repeated stacks of hydrophilic domains of the polymeric system is expected via self-assembly. However, the very large aspect ratio of typical SWNTs can be a problem for SWNTs to be selectively confined in domains of very narrow thicknesses compared to the length of SWNTs. It is, however, difficult to directly observe SWNTs selectively distributed in polymeric systems. Most common microscopy techniques such as AFM, TEM, or SEM have their specific disadvantages in visualizing SWNTs within a polymer matrix.[34] In this study, contrast variation SANS is used to identify the location of SWNTs within the polymeric systems. Since the neutron scattering contrast between the hydrophilic and the hydrophobic domains is changed by the selective distribution of SWNTs in one of the domains, variations of SANS intensities of the ternary system with different amount of SWNTs will allow us to identify the selective distribution of SWNT in the polymeric system. To our knowledge, this is

*Corresponding author. E-mail: sungmin@kaist.ac.kr.

Published on Web 05/19/2010

Table 1. Weight Fractions of Hydrogenated Solvents in *p*-Xylene and Water and Calculated Average SLDs of Apolar ($\overline{\rho}_{apolar}$) and Polar ($\overline{\rho}_{apolar}$) Domains for P84/Water/*p*-Xylene Ternary Systems at Lamellar Phase

	p-xylene-*n*: *p*-xylene-*d* (weight ratio)	H_2O:D_2O (weight ratio)	$\overline{\rho}_{apolar}$ ($\times 10^{10}$ cm^{-2})	$\overline{\rho}_{polar}$ ($\times 10^{10}$ cm^{-2})
positive contrast	0:100	46.6:53.4	3.00	2.27
negative contrast	0:100	0:100	3.00	4.63

the first experimental study to show the selective distribution of SWNTs in polymeric systems by a contrast variation SANS technique.

Materials and Experimental Methods

Materials. Superpurified HiPco single-walled carbon nanotubes (SWNT, purity >98 wt %) were purchased from Carbon Nanotechnologies Inc., and Pluronic P84, $(EO)_{19}(PO)_{43}(EO)_{19}$, block copolymer was provided by BASF as a gift and was used as received. Cetyltrimethylammonium hydroxide (CTAOH) was purchased from Fluka. 4-Vinylbenzoic acid was purchased from Aldrich. Water-soluble free-radical initiator VA-044 (2,2′-azobis-[2-(2-imidazolin-2-yl)propane] dihydrochloride) was purchased from Wako Chemicals. Deionized water (Milli-Q, Millipore) was used for hydrogenated water (H_2O). Hydrogenated *p*-xylene (or *p*-xylene-*n*) of purity >99% was purchased from Sigma-Aldrich. Deuterated water (D_2O, 99.9 atom % D) and deuterated *p*-xylene (*p*-xylene-d_{10}, $C_6D_4(CD_3)_2$, >98 atom % D) were purchased from Cambridge Isotope Laboratories. Cetyltrimethylammonium 4-vinylbenzoate (CTVB) was synthesized by neutralization of 4-vinylbenzoic acid in the presence of a slight stoichiometric excess of CTAOH followed by repeated crystallization.[35] The polymeric system in the lamellar phase was prepared at a composition of P84/water/*p*-xylene of 40/40/20 ratio by weight at room temperature.

Functionalization of SWNTs. Functionalized SWNTs (*p*-SWNTs) whose surfaces are hydrophilically modified were prepared as described elsewhere.[33] Briefly, HiPco SWNTs (2 mg/mL) were mixed in water with the cationic surfactant CTVB (5 mg/mL) which has polymerizable counterions (4-vinylbenzoate). The mixture of SWNT and CTVB was sonicated for 1 h to exfoliate bundled SWNTs and produce individually isolated SWNTs with an adsorbed monolayer of CTVB. The CTVB monolayer on SWNT surface was "locked in" by *in situ* free-radical polymerization of the counterions of CTVB at 60 °C using the free-radical initiator VA-044. The polymerized mixture was ultracentrifuged (ca. 111 000*g*) for 4 h to separate isolated SWNTs from bundled ones, and the upper ca. 70% of the solution, which was a homogeneous dispersion of SWNTs, was decanted and freeze-dried. In the previous study, SANS measurement of *p*-SWNT in D_2O showed that isolated SWNTs of average diameter, 1.0 nm, are cylindrically encapsulated by polymerized surfactant monolayers whose thickness is about 2.0 nm, resulting in 5.0 nm for the diameter of *p*-SWNTs.[33] The average length of *p*-SWNTs were found to be around 500 nm by atomic force microscope measurements.[33]

Contrast Variation Small-Angle Neutron Scattering. The P84/water/*p*-xylene ternary system at lamellar phase can be divided into polar (PEO + water) and apolar (PPO + *p*-xylene) domains.[36,37] If SWNTs are selectively distributed in either polar or apolar domains, the average neutron scattering length density (SLD) of the corresponding domain will be changed, resulting in a change in the scattering intensity. The changes of the scattering intensity due to the selective distribution of SWNTs can be described as follows.

The scattering intensity of the first-order Bragg peak (*I*) from the simple two phase lamellar system is proportional to the square of the neutron scattering contrast ($\Delta\rho$) which is the difference between the average neutron SLDs of the apolar domain ($\overline{\rho}_{polar}$) and the polar domain ($\overline{\rho}_{polar}$) and can be written as

$$I = C(\overline{\rho}_{apolar} - \overline{\rho}_{polar})^2 = C(\Delta\rho)^2 \quad (1)$$

where *C* is a proportional coefficient.[38]

If both $\overline{\rho}_{apolar}$ and $\overline{\rho}_{polar}$ are greater than the SLD of *p*-SWNTs, selective distribution of *p*-SWNTs in either of the domains will reduce the average SLD of the corresponding domain. This condition is satisfied in our experiments (see Table 1). This will result in either an increase or a decrease of the scattering intensities depending on the relative SLDs of the two domains before the addition of *p*-SWNTs. When the average SLDs before the addition of *p*-SWNTs satisfy $\overline{\rho}_{apolar} > \overline{\rho}_{polar}$, the scattering intensity will increase if *p*-SWNTs are selectively distributed in the polar domain and will decrease if *p*-SWNTs are selectively distributed in the apolar domain (Figure 1a). On the other hand, when the average SLDs before the addition of *p*-SWNTs satisfy $\overline{\rho}_{apolar} < \overline{\rho}_{polar}$, the scattering intensity will decrease if *p*-SWNTs are selectively distributed in the polar domain and will increase if *p*-SWNTs are selectively distributed in the apolar domain (Figure 1b). Therefore, the change of scattering intensities of the P84/water/*p*-xylene ternary systems with different amount of *p*-SWNTs, which are prepared with the two different scattering contrast conditions ($\overline{\rho}_{apolar} > \overline{\rho}_{polar}$ or $\overline{\rho}_{apolar} < \overline{\rho}_{polar}$), will allow us to identify the selective distribution of *p*-SWNTs in the lamellar phase. Here, we denote the scattering contrast conditions, $\overline{\rho}_{apolar} - \overline{\rho}_{polar} > 0$ and $\overline{\rho}_{apolar} - \overline{\rho}_{polar} < 0$, as a positive contrast condition and a negative contrast condition, respectively.

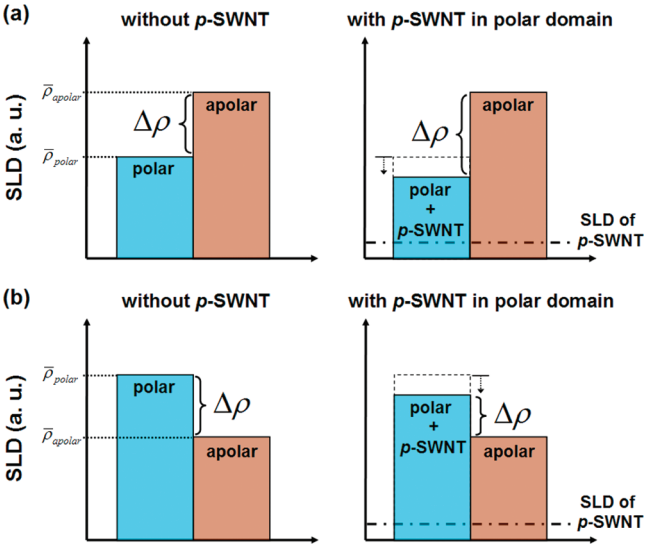

Figure 1. Schematics showing the average SLD changes in two different scattering contrast conditions assuming that *p*-SWNTs are selectively distributed in the polar domains. (a) When $\overline{\rho}_{apolar} > \overline{\rho}_{polar}$ (positive contrast condition), the scattering contrast ($\Delta\rho$) will increase if *p*-SWNTs are selectively distributed in the polar domain. (b) When $\overline{\rho}_{apolar} < \overline{\rho}_{polar}$ (negative contrast condition), the scattering contrast ($\Delta\rho$) will decrease if *p*-SWNTs are selectively distributed in the polar domain. The SLDs of $\overline{\rho}_{apolar}$ and $\overline{\rho}_{polar}$ are always higher than the SLD of *p*-SWNT (dash-dotted line).

Preparation of Mixtures of P84/Water/*p*-Xylene Ternary Systems with *p*-SWNTs. P84/water/*p*-xylene (40/40/20 by weight) ternary mixtures are prepared in two different neutron scattering contrast conditions. For each ternary system, the concentration of *p*-SWNT in water is varied from 0 to 4 wt % (0, 1, 2, 3, and 4 wt % in water). To prepare ternary systems with positive and negative neutron scattering contrasts, the SLD of water was varied by mixing H_2O and D_2O appropriately (Table 1) while the SLD of the *p*-xylene was kept constant by using deuterated *p*-xylene (*p*-xylene-d_{10}) for both scattering

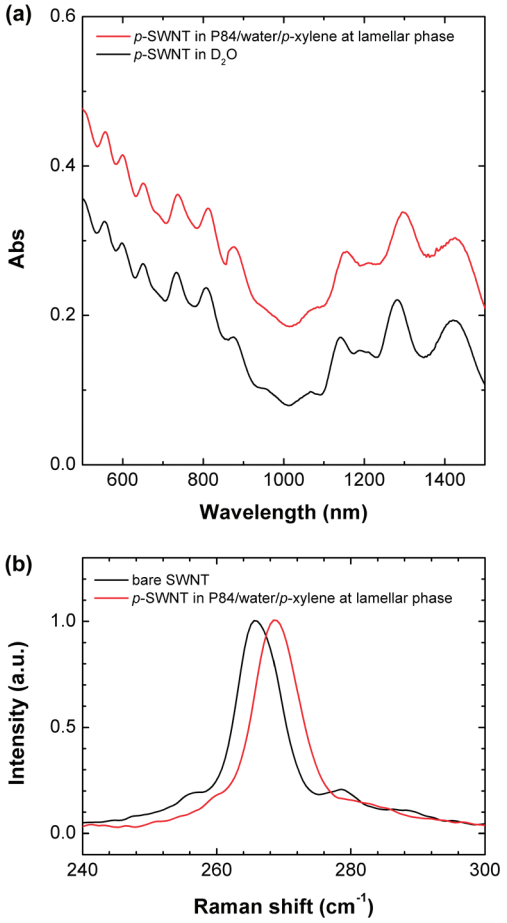

Figure 2. (a) UV−vis−NIR absorption spectra of *p*-SWNTs in P84/water/*p*-xylene lamellar phase (red) and in water (black). The red line is vertically shifted for visual clarity. (b) Raman shifts from *p*-SWNTs in P84/water/*p*-xylene lamellar phase (red) is shown with the Raman shift from raw bundled SWNTs (black). Raman intensities are normalized to 1 for the peak near 270 cm^{-1} for visual clarity. Both the UV−vis−NIR and Raman spectra measurements were performed on the P84/water/*p*-xylene ternary system mixed with 3 wt % *p*-SWNTs in water.

contrasts. The calculated average SLDs of polar and apolar domains are listed in Table 1. The SLDs of PEO,[39] PPO,[39] *p*-SWNT, H_2O, D_2O, *p*-xylene-*n*, and *p*-xylene-d_{10} are 0.57, 0.35, 0.53, −0.57, 6.33, 0.77, and 5.84×10^{10} cm^{-2}, respectively. The SLDs of water and *p*-xylene which were prepared as described above also ensure that the SLDs of $\overline{\rho}_{apolar}$ and $\overline{\rho}_{polar}$ are always higher than the SLD of *p*-SWNT (0.53×10^{10} cm^{-2}). The samples were centrifuged repeatedly in alternating directions for several days to facilitate mixing and kept at room temperature for a few days. The P84/water/*p*-xylene ternary systems mixed with various concentrations of *p*-SWNTs did not show any visual aggregation after several days of alternative centrifuge mixing (Supporting Information, Figure S1).

UV−vis−NIR Measurements. A PerkinElmer LAMBDA 750 UV−vis−NIR spectrometer with quartz cells of 2 mm beam path length was used to measure absorption spectra of *p*-SWNTs in P84/water/*p*-xylene and D_2O.

Raman Spectra Measurements. Raman spectra of *p*-SWNTs in P84/water/*p*-xylene and pristine SWNT were obtained using FT-Raman spectroscopy (Bruker, RFS-100) with laser excitation 1064 nm and resolution 1 cm^{-1}.

Small-Angle Neutron Scattering Measurements. SANS measurements were performed using the NG7 30 m SANS instrument at the National Institute of Standards and Technology (NIST) in Gaithersburg, MD.[40] Neutrons of wavelength $\lambda = 6$ Å with a full width half-maximum $\Delta\lambda/\lambda = 11\%$ were used. A single sample-to-detector distance of 4 m was used to cover the q range of 0.012 $Å^{-1} < q < 0.152$ $Å^{-1}$ where $q = (4\pi/\lambda)\sin(\theta/2)$ is the magnitude of the scattering vector and θ is the scattering angle. Sample scattering was corrected for background and empty cell scattering and the sensitivity of individual detector pixels. The corrected data sets were placed on an absolute scale using the data reduction software provided by NIST[41] through the direct beam flux method. All the SANS measurements were carried out at 25 °C using quartz cells of 1 mm path length.

Results and Discussion

The UV−vis−NIR spectrum of the *p*-SWNTs mixed with the P84/water/*p*-xylene in lamellar phase is essentially identical as that of *p*-SWNTs dispersed in water showing sharp van Hove transition peaks (Figure 2a), which indicates that most of the SWNTs in the P84/water/*p*-xylene ternary system exist in an individually isolated form without forming aggregates.[42] In addition, the radial breathing modes of the Raman spectrum of the *p*-SWNTs mixed with the P84/water/*p*-xylene system shows ca. 4 cm^{-1} shift to higher frequency compared to that of the bundled SWNTs in water (Figure 2b), which further confirms the existence of the debundled and individually isolated SWNTs in the P84/water/*p*-xylene systems.[43]

The SANS intensities of P84/water/*p*-xylene (40/40/20 by weight) mixed with different amount of *p*-SWNTs are summarized in Figure 3 for each scattering contrast condition. Since the average scattering contrast between the polar and apolar domains of the negative contrast samples is larger than that of the positive contrast samples, the scattering intensities of the first-order Bragg peak (which is sensitive to the average scattering contrast[38]) from the negative contrast samples are larger than those from the positive contrast samples. However, the scattering intensity of the second-order Bragg peak is approximately the same for the two contrast conditions, which can be explained by the detailed subdomain structures of the samples as previously reported.[38] The peak position ratios of all the positive and negative contrast samples with and without *p*-SWNTs are 1:2, indicating that the underlying lamellar structures are maintained regardless of the neutron contrast variation or the addition of *p*-SWNTs. As the concentration of *p*-SWNTs is increased, the intensity of the first-order Bragg peak from the negative contrast samples monotonically decreases, which suggests that *p*-SWNTs are selectively distributed in the polar domain reducing the scattering contrast. However, the intensity of the first-order Bragg peak from the positive contrast samples, which is expected to increase if *p*-SWNTs are selectively distributed in the polar domain, slightly decreases with the addition of *p*-SWNTs, but more slowly than that of the negative contrast samples. The periodicities of the lamellar structures without *p*-SWNTs are 13.8 and 13.6 nm for the positive and negative contrast samples, respectively. Considering that all the samples were prepared on a weight basis, the small difference in the periodicity can be attributed to the difference in mass densities of H_2O and D_2O (Figure 3). As the concentration of *p*-SWNT is increased, the scattering peak position is slightly shifted to higher q, indicating that the periodicity of lamellar structures is slightly decreased. This may be attributed to redistribution of solvent by the inclusion of *p*-SWNTs.[44] The increase (up to ca. 7%) of the scattering peak width is also observed as the concentration of *p*-SWNT is increased, indicating that positional disorder or defects of lamellar structures has been increased by the addition of *p*-SWNT. Analysis of the first Bragg peaks of measured SANS intensities[45,46] suggests that the standard deviation of positional disorder distribution of the lamellar structure is increased by up to ca. 0.75 nm (from 3.08 to 3.83 nm) by the addition of *p*-SWNTs (Supporting Information). This perturbation or defects of lamellar structures may contribute to stabilize *p*-SWNT within the lamellar structures.[47]

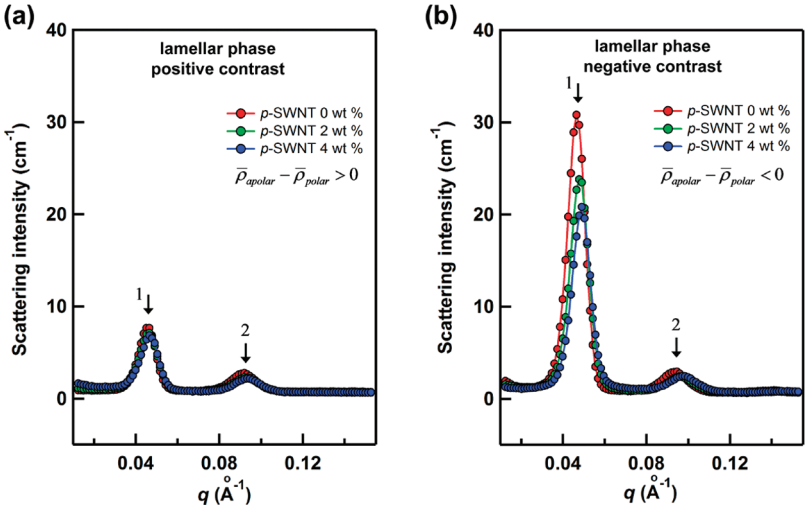

Figure 3. Scattering intensities of P84/water/*p*-xylene lamellar phase mixed with *p*-SWNTs with (a) a positive scattering contrast condition and (b) a negative scattering contrast condition. The concentrations of *p*-SWNTs are indicated as weight percent in water. Relative peak positions are indicated.

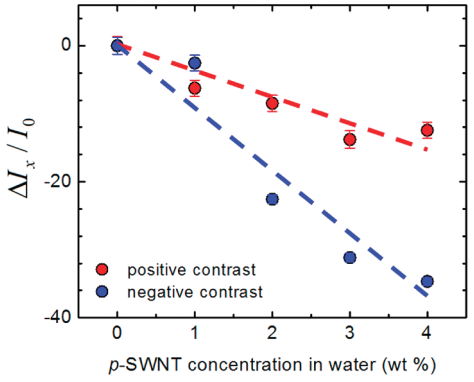

Figure 4. Relative scattering intensity changes of the first Bragg peak from P84/water/*p*-xylene ternary systems mixed with different amount of *p*-SWNTs. Dashed lines are guides for the eye.

To understand the variation of scattering intensities with addition of *p*-SWNTs more quantitatively, the relative scattering intensity changes ($\Delta I_x/I_0$) of the first-order Bragg peak, which is sensitive to the average scattering contrast between the polar and apolar domains,[38] are plotted against the concentration of *p*-SWNT in water (Figure 4). Here, $\Delta I_x = I_x - I_0$, where I_x is the scattering intensity of the first-order Bragg peak from the sample with x wt % *p*-SWNTs in water and I_0 is that of the sample without *p*-SWNT. As the concentration of *p*-SWNT in water is increased from 0 to 4 wt %, $\Delta I_x/I_0$ decreases to ca. −33% and ca. −12% for the negative ($\bar{\rho}_{apolar} - \bar{\rho}_{polar} < 0$) and positive ($\bar{\rho}_{apolar} - \bar{\rho}_{polar} > 0$) contrast samples, respectively. In the negative contrast sample with 4 wt % *p*-SWNT in water, if *p*-SWNTs (with a SLD of 0.53×10^{10} cm^{-2}) are selectively distributed in the polar domain, the calculated average SLD of the polar domain mixed with *p*-SWNTs is 4.46×10^{10} cm^{-2}, which is smaller than the SLD of the polar domain before adding *p*-SWNTs (4.63×10^{10} cm^{-2}). This decrease of polar domain SLD reduces the scattering contrast. A similar calculation is performed for the positive contrast sample with 4 wt % *p*-SWNT in water, resulting in the average SLD of the polar domain mixed with *p*-SWNTs (2.20×10^{10} cm^{-2}), which is smaller than the SLD of the polar domain before adding *p*-SWNTs (2.27×10^{10} cm^{-2}). This decrease of polar domain SLD increases the scattering contrast. The changes of scattering intensity due to the change of scattering contrast by adding *p*-SWNTs (4 wt % in water) are calculated to be ca. −20% (decrease) and ca. +19% (increase) for the negative and positive contrast samples, respectively. However, the measured scattering intensity of the negative contrast sample shows much larger decrease (ca. −33%) than the calculated one, and that of the positive sample shows decrease rather than increase. It should be noted, however, that the intensity decrease of the negative contrast sample is always larger than that of the positive contrast sample. This may indicate that there is another mechanism (which is independent of the contrast conditions) that decreases the scattering intensity by the addition of *p*-SWNTs.

This decrease in the scattering intensity can be explained as follows. From the lamellar periodicity (13.6 nm) and the polar volume fraction (ca. 0.54) of the negative contrast sample without *p*-SWNTs, the polar and the apolar domain thicknesses are calculated to be 7.4 and 6.2 nm, respectively. A recent study of P84/water/*p*-xylene ternary systems in the lamellar phase[38] showed that a thin (ca. 0.6 nm) water-rich layer exists in the middle of the polar domain. Considering that the diameter of *p*-SWNT[33] (5 nm) is comparable to the thicknesses of the polar domain, the inclusion of *p*-SWNTs in the polar domain will disturb the polar/apolar interfaces as shown in Figure 5, which can make the polar/apolar domain interfaces effectively diffuse and lead to the decrease of scattering intensities. Therefore, the additional intensity decrease in the negative contrast sample with 4 wt % *p*-SWNT in water can be attributed to the diffuse interface induced by the inclusion of *p*-SWNTs in the polar domains. Since the scattering intensity decrease due to the diffuse interface is expected to occur in the positive contrast samples as well, the scattering intensity of the positive contrast sample (which was supposed to increase with addition of *p*-SWNTs) may decrease if the effect of the diffuse interface is large enough.

To identify the contribution of the *p*-SWNT-induced diffuse interface to the decrease of scattering intensity, the measured scattering intensity change of the negative contrast condition (ca. −33%) is compared with the expected scattering intensity change due to *p*-SWNT (4 wt % in water) induced contrast change (ca. −20%) as follows. The measured scattering intensity of the first Bragg peak, I^{meas}, can be described by the multiplication of two independent terms as $I^{meas} = I^{cont} f_{diff}$, where I^{cont} is the scattering intensity of the first Bragg peak determined by the average scattering contrast between the polar and the apolar domains with sharp interfaces, and f_{diff} is a factor describing the scattering intensity decrease due to the *p*-SWNT-induced diffuse interfaces. $f_{diff} = 1$ when there are no *p*-SWNTs in the mixture. In the case of a Gaussian bilayer model, which is one of the

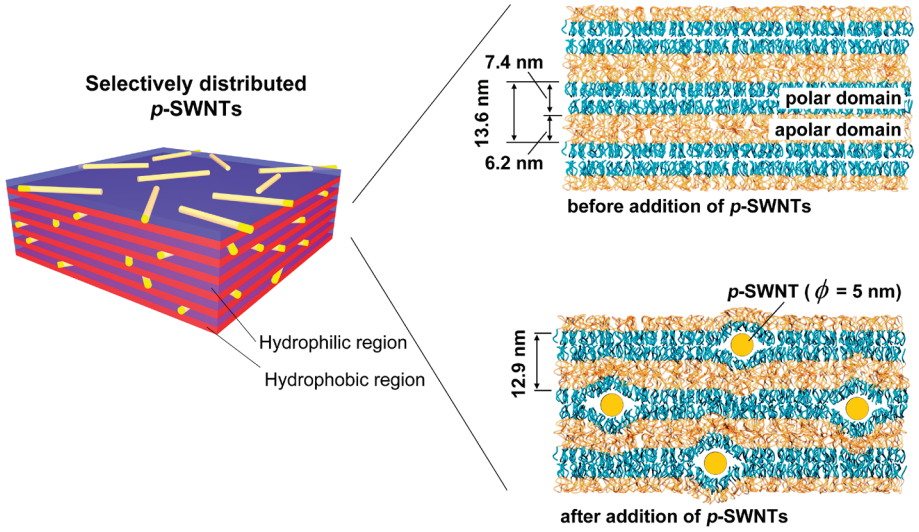

Figure 5. Schematics for the selective distribution of *p*-SWNTs in a P84/water/*p*-xylene lamellar phase. Any periodic or orientational correlations among *p*-SWNTs in each polar domain are not observed in the current SANS data. Therefore, *p*-SWNTs in polar domains are assumed to be randomly distributed. The dimensions indicated in the figure are for the negative contrast samples without and with *p*-SWNTs (4 wt % in water).[44]

examples describing diffuse interfaces, f_{diff} has an exponential form.[48] Since the effect of diffuse interface is purely structural, the factor f_{diff} is assumed to be independent of the scattering contrast conditions. On the basis of this assumption, $f_{diff} \approx 0.83$ can be obtained from the experimentally measured scattering intensity variation with 4 wt % *p*-SWNTs in water (ca. −33%) and the expected scattering intensity variation (ca. −20%) which is calculated from the scattering contrast changes due to addition of *p*-SWNTs (Supporting Information). Since the effect of *p*-SWNT-induced diffuse interface is expected to be same for the positive contrast samples, it can be assumed that f_{diff} obtained from the negative contrast sample is same for the positive contrast sample. When the measured scattering intensity change (ca. −12%) of the positive contrast sample is corrected for the effect of *p*-SWNT-induced diffuse interface using $f_{diff} \approx 0.83$, the scattering intensity change due to the *p*-SWNT-induced average contrast change becomes ca. 6% (Supporting Information). It should be noted that once it is corrected for the diffuse interface effect, the scattering intensity change of the positive contrast sample with the addition of *p*-SWNTs is positive as expected for selective distribution of *p*-SWNT in polar domains. The corrected scattering intensity change (= ca. 6%) is, however, smaller than the expected value (ca. 19%). This discrepancy may be attributed to the fact that the average SLD of the polar domain was calculated by assuming homogeneous mixture of *p*-SWNTs, PEO, and water, while the polar domains containing *p*-SWNTs with a diameter of 5 nm and a length of ca. 500 nm are not truly homogeneous in the length scale of SANS measurements.

Once the effect of *p*-SWNT-induced diffuse interface is corrected, the neutron scattering intensity of the first-order Bragg peak increases with addition of *p*-SWNTs in the positive contrast samples and decreases in the negative contrast samples, which is consistent with the expectation for selective distribution of *p*-SWNTs in the polar domains of the ternary systems. Therefore, this confirms that *p*-SWNTs which are functionalized to have hydrophilic surfaces are selectively distributed in the polar domains of lamellar structures of P84/water/*p*-xylene. It should be noted that while the diameter (5 nm) of *p*-SWNT is comparable to the thickness of polar domain (7.4 nm), its length (ca. 500 nm) is ca. 70 times larger than the thickness of polar domain. This suggests that properly functionalized anisotropic nanoparticles can be selectively incorporated into a specific domain of polymeric lamellar structures even if one of the dimensions of the nanoparticle is far larger than corresponding domain thickness (the other dimension is comparable to the domain thickness).

The *p*-SWNTs confined in the polar domains of lamellar structures can be considered rods confined in two-dimensional space. The Onsager's mean field model applied to an infinite two-dimensional system of rods predicts that the isotropic−nematic transition occurs at a critical area fraction of rods given as $\varphi^* = 3\pi/2(L/D)^{-1}$, where L and D are the length and diameter of rods.[49,50] For the *p*-SWNTs (L/D = ca. 100) used in this study, $\varphi^* = 0.047$. If it is assumed that all *p*-SWNTs (4 wt % in water) are confined in the polar domain without overlapping, the area fraction of *p*-SWNT is calculated to be 0.054, which is slightly larger than φ^*. Therefore, there is some possibility of orientational ordering of *p*-SWNTs in the two-dimensional polar domain. However, it should be noted that while the two-dimensional boundaries in Onsager's mean field model are hard walls, those in the polar domain of lamellar structures are soft walls which provide different rod−wall interactions. This difference of walls makes the prediction of isotropic−nematic transition of *p*-SWNTs in two-dimensional polar domain rather difficult. To identify the two-dimensional isotropic−nematic transition of *p*-SWNTs, a further investigation would be needed.

Conclusion

We have investigated the distribution of hydrophilically functionalized SWNTs in the P84/water/*p*-xylene lamellar phase using contrast variation SANS measurements. The neutron scattering intensity of the first-order Bragg peak, after correcting for the effect of *p*-SWNT-induced diffuse interface, was increased with addition of *p*-SWNTs in the positive contrast samples and decreased in the negative contrast samples, which confirmed that *p*-SWNTs are selectively distributed in the polar domains of the P84/water/*p*-xylene lamellar phase. The selective distribution of *p*-SWNTs was driven by the hydrophilic surfaces of *p*-SWNTs which provide selective affinity to the polar domains of the block copolymer system. This suggests that block copolymer systems can be used as a simple and easy route to fabricate selectively distributed SWNT composites, providing new opportunities for the applications of SWNTs.

Acknowledgment. This work was supported by National Research Foundation grants funded by the Ministry of Education, Science and Technology of the Korean government

(No. 2010-0000859, No. 2010-0017424, and No. 2010-0000133) and a grant from the Construction Technology Innovation Program funded by the Ministry of Land, Transportation and Maritime Affairs of the Korean government. This work utilized facilities supported in part by the National Science Foundation under Agreement DMR-0454672. The mention of commercial products does not imply endorsement by NIST, nor does it imply that the materials or equipment identified are necessarily the best available for the purpose.

Supporting Information Available: Analysis of scattering peak broadening due to addition of *p*-SWNTs; correcting the effect of *p*-SWNT-induced diffuse interface. This material is available free of charge via the Internet at http://pubs.acs.org.

References and Notes

(1) Park, S.; Lim, J.-H.; Chung, S.-W.; Mirkin, C. A. *Science* **2004**, *303*, 348–351.
(2) Titov, A. V.; Král, P. *Nano Lett*. **2008**, *8*, 3605–3612.
(3) Li, X.; Zhang, L.; Wang, X.; Shimoyama, I.; Sun, X.; Seo, W.-S.; Dai, H. *J. Am. Chem. Soc*. **2007**, *129*, 4890–4891.
(4) Dresselhaus, M. S.; Dresselhaus, G.; Avouris, P. *Carbon Nanotubes: Synthesis, Structure, Properties, and Applications*; Springer-Verlag: Berlin, 2001.
(5) Saito, R.; Dresselhaus, G.; Dresselhaus, M. S. *Physical Properties of Carbon Nanotubes*; Imperial College Press: London, 1998.
(6) Cao, Q.; Kim, H.-s.; Pimparkar, N.; Kulkami, J. P.; Wang, C.; Shim, M.; Roy, K.; Alam, M. A.; Rogers, J. A. *Nature* **2008**, *454*, 495–500.
(7) Lemieux, M. C.; Roberts, M.; Barman, S.; Jin, Y. W.; Kim, J. M.; Bao, Z. *Science* **2008**, *321*, 101–104.
(8) Li, J.; Lu, Y.; Ye, Q.; Cinke, M.; Han, J.; Meyyappan, M. *Nano Lett*. **2003**, *3*, 929–933.
(9) Besteman, K.; Lee, J.-O.; Wiertz, F. G. M.; Heering, H. A.; Dekker, C. *Nano Lett*. **2003**, *3*, 727–730.
(10) Barone, P. W.; Baik, S.; Heller, D. A.; Strano, M. S. *Nat. Mater*. **2005**, *4*, 86–92.
(11) Futaba, D. N.; Hata, K.; Yamada, T.; Hiraoka, T.; Hayamizu, Y.; Kakudate, Y.; Tanaike, O.; Hatori, H.; Yumura, M.; Iijima, S. *Nat. Mater*. **2006**, *5*, 987–994.
(12) Zhang, H.; Cao, G.; Wang, Z.; Yang, Y.; Shi, Z.; Gu, Z. *Nano Lett*. **2008**, *8*, 2664–2668.
(13) Veedu, V. P.; Cao, A.; Li, X.; Ma, K.; Soldano, C.; Kar, S.; Ajayan, P. M.; Ghasemi-Nejhad, M. N. *Nat. Mater*. **2006**, *5*, 457–462.
(14) Coleman, J. N.; Khan, U.; Gun'ko, Y. K. *Adv. Mater*. **2006**, *18*, 689–706.
(15) Yan, Y.; Chan-Park, M. B.; Zhang, Q. *Small* **2007**, *3*, 24–42.
(16) Islam, M. F.; Alsayed, A. M.; Dogic, Z.; Zhang, J.; Lubensky, T. C.; Yodh, A. G. *Phys. Rev. Lett*. **2004**, *92*, 088303.
(17) Simmons, T. J.; Hashim, D.; Vajtai, R.; Ajayan, P. M. *J. Am. Chem. Soc*. **2007**, *129*, 10088–10089.
(18) Kamat, P. V.; Thomas, K. G.; Barazzouk, S.; Girishkumar, G.; Vinodgopal, K.; Meisel, D. *J. Am. Chem. Soc*. **2004**, *126*, 10757–10762.
(19) Bates, F. S.; Fredrickson, G. H. *Phys. Today* **1999**, *52*, 32–38.
(20) Discher, D. E.; Eisenberg, A. *Science* **2002**, *297*, 967–973.
(21) Vaia, R. A.; Maguire, J. F. *Chem. Mater*. **2007**, *19*, 2736–2751.
(22) Yang, C.-S.; Awschalom, D. D.; Stucky, G. D. *Chem. Mater*. **2002**, *14*, 1277–1284.
(23) Balazs, A. C.; Emrick, T.; Russell, T. P. *Science* **2006**, *314*, 1107–1110.
(24) Bockstaller, M. R.; Lapetnikov, Y.; Margel, S.; Thomas, E. L. *J. Am. Chem. Soc*. **2003**, *125*, 5276–5277.
(25) Chiu, J. J.; Kim, B. J.; Kramer, E. J.; Pine, D. J. *J. Am. Chem. Soc*. **2005**, *127*, 5036–5037.
(26) Lin, Y.; Boker, A.; He, J.; Sill, K.; Xiang, H.; Abetz, C.; Li, X.; Wang, J.; Emrick, T.; Long, S.; Wang, Q.; Balazs, A.; Russell, T. P. *Nature* **2005**, *434*, 55–59.
(27) Deshmukh, R. D.; Liu, Y.; Composto, R. J. *Nano Lett*. **2007**, *7*, 3662–3668.
(28) Thompson, R. B.; Ginzburg, V. V.; Matsen, M. W.; Balazs, A. C. *Science* **2001**, *292*, 2469–2472.
(29) Sides, S. W.; Kim, B. J.; Kramer, E. J.; Fredrickson, G. H. *Phys. Rev. Lett*. **2006**, *96*, 250601.
(30) Kang, H.; Detcheverry, F. A.; Mangham, A. N.; Stoykovich, M. P.; Daoulas, K. C.; Hamers, R. J.; Muller, M.; Pablo, J. J. d.; Nealey, P. F. *Phys. Rev. Lett*. **2008**, *100*, 148303.
(31) Sknepnek, R.; Anderson, J. A.; Lamm, M. H.; Schmalian, J.; Travesset, A. *ACS Nano* **2008**, *2*, 1259–1265.
(32) Alexandridis, P.; Olsson, U.; Lindman, B. *Langmuir* **1998**, *14*, 2627–2638.
(33) Kim, T.-H.; Doe, C.; Kline, S. R.; Choi, S.-M. *Adv. Mater*. **2007**, *19*, 929–933.
(34) Loos, J.; Alexeev, A.; Grossiord, N.; Koning, C. E.; Regev, O. *Ultramicroscopy* **2005**, *104*, 160–167.
(35) Kline, S. R. *Langmuir* **1999**, *15*, 2726–2732.
(36) Alexandridis, P.; Nivaggioli, T.; Hatton, T. A. *Langmuir* **1995**, *11*, 1468–1476.
(37) Alexandridis, P.; Olsson, U.; Lindman, B. *Macromolecules* **1995**, *28*, 7700–7710.
(38) Doe, C.; Jang, H.-S.; Kline, S. R.; Choi, S.-M. *Macromolecules* **2009**, *42*, 2645–2650.
(39) Chen, S. H.; Liao, C.; Fratini, E.; Baglioni, P.; Mallamace, F. *Colloids Surf., A* **2001**, *183*−*185*, 95–111.
(40) Glinka, C. J.; Barker, J. G.; Hammouda, B.; Krueger, S.; Moyer, J. J.; Orts, W. J. *J. Appl. Crystallogr*. **1998**, *31*, 430.
(41) Kline, S. R. *J. Appl. Crystallogr*. **2006**, *39*, 895–900.
(42) O'Connell, M. J.; Bachilo, S. M.; Huffman, C. B.; Moore, V. C.; Strano, M. S.; Haroz, E. H.; Rialon, K. L.; Boul, P. J.; Noon, W. H.; Kittrell, C.; Ma, J.; Hauge, R. H.; Weisman, R. B.; Smalley, R. E. *Science* **2002**, *297*, 593–596.
(43) Yan, L. Y.; Poon, Y. F.; Chan-Park, M. B.; Chen, Y.; Zhang, Q. *J. Phys. Chem. C* **2008**, *112*, 7579–7587.
(44) The inclusion of *p*-SWNTs, however, may not only induce diffusive interfaces but also reduce the periodicity of the lamellar structure because withdrawal of water molecules from the regions where there are no *p*-SWNTs can be occurred to hydrate *p*-SWNTs and to increase the water-gap spaces near the *p*-SWNTs.
(45) Podgornik, R.; Rau, D. C.; Parsegian, V. A. *Macromolecules* **1989**, *22*, 1780–1786.
(46) Guinier, J. *X-ray Diffraction in Crystals, Imperfect Crystals and Amorphous Bodies*; W.H. Freeman: San Francisco, 1963.
(47) Listak, J.; Bockstaller, M. R. *Macromolecules* **2006**, *39*, 5820–5825.
(48) Wiener, M. C.; White, S. H. *Biophys. J*. **1991**, *59*, 162–173.
(49) Kayser, R. F.; Raveche, H. J. *Phys. Rev. A* **1978**, *17*, 2067–2072.
(50) Galanis, J.; Harries, D.; Sackett, D. L.; Losert, W.; Nossal, R. *Phys. Rev. Lett*. **2006**, *96*, 028002.